MOLECULAR AND CELLULAR BIOLOGY, July 2009, p. 4014–4023 Vol. 29, No. 14
0270-7306/09/$08.00+0 doi:10.1128/MCB.01582-08

Functional Redundancy of Yeast Proteins Reh1 and Rei1 in Cytoplasmic 60S Subunit Maturation▽

K. Mark Parnell* and Brenda L. Bass*

Department of Biochemistry and Howard Hughes Medical Institute, University of Utah School of Medicine, 15 North Medical Drive East, Room 4800, Salt Lake City, Utah 84112-5650

Received 8 October 2008/Returned for modification 8 December 2008/Accepted 1 May 2009

The biogenesis of the large (60S) ribosomal subunit in eukaryotes involves nucleolar, nucleoplasmic, and cytoplasmic steps. The cytoplasmic protein Rei1, found in all eukaryotes, was previously shown to be necessary for the nuclear reimport of 60S subunit export factor Arx1. In this study we investigate the function of Reh1, a protein with high sequence similarity to Rei1. We demonstrate an overlapping function for Reh1 and Rei1 in the cytoplasmic maturation of the 60S subunit that is independent of Arx1 recycling. We observe that strains lacking both Reh1 and Rei1 accumulate salt-labile 60S subunits, suggesting that Reh1/Rei1 is necessary for the cytoplasmic 60S subunit to adopt its mature, stable form.

Eukaryotic ribosomes are the products of a highly conserved assembly process involving more than 170 *trans*-acting biogenesis factors, around 75 ribosomal proteins (r-proteins), and four rRNAs (8, 10, 42). The small (40S) and large (60S) ribosomal subunits are assembled independently, first in the nucleolus and then the nucleoplasm, followed by export to the cytoplasm. Evidence suggests that the newly exported cytoplasmic pre-60S particle requires a slow maturation step before entering the pool of translating ribosomes (33, 40, 44). The exact nature of cytoplasmic 60S maturation is not well understood but is thought to involve the following steps: (i) the loading of a number of r-proteins, including Rpp0, Rpl7, Rpl10, and Rpl24; (ii) the dissociation and reimport of a small number of nonribosomal factors to the nucleus; and (iii) stabilizing structural rearrangements (43).

The cytoplasmic protein Rei1 is necessary for the nuclear recycling of Arx1 (19, 27), a 60S subunit export factor (5, 20). Rei1 is conserved in all eukaryotes but absent from archaea and bacteria, suggesting an important eukaryote-specific cellular function (11). In *Saccharomyces cerevisiae* and a limited number of fungal organisms, an Rei1-related factor named Reh1 is also present. Reh1, like Rei1, is a cytoplasmic protein (18) with three U1-type C_2H_2 zinc fingers (InterPro number IPR003604), and the two proteins share 34% sequence identity and 54% sequence similarity. Previous studies indicated a degree of functional redundancy between Reh1 and Rei1, as a double deletion of *REH1* and *REI1* results in a synthetic growth defect (22), and overexpression of *REH1* can partially suppress the *rei1*Δ cold-sensitive growth phenotype (22, 27). However, the overlapping functions of Reh1 and Rei1 were suggested to be unrelated to 60S subunit ribosome biogenesis based on several observations: (i) polysome profiles and rRNA processing were not affected in the *reh1*Δ strain (26, 27); (ii) depletion of Reh1 in the *rei1*Δ background did not significantly increase rRNA maturation defects observed in *rei1*Δ cells (26); and (iii) 60S subunit export was not affected by depletion of Reh1 in *rei1*Δ cells (26).

Here, we investigate the overlapping functions of Reh1 and Rei1 and find strong evidence that Reh1 is involved in cytoplasmic 60S subunit biogenesis. Like Rei1, Reh1 is associated with newly synthesized 60S subunits and cytoplasmic biogenesis factors. Further, the synthetic growth defect observed in *reh1*Δ *rei1*Δ strains is independent of Arx1 recycling and correlates with severe defects in polysome profiles, subunit joining, and 60S subunit stability. We conclude that Rei1, in addition to its role in Arx1 recycling, acts redundantly with Reh1 to directly promote a stabilizing structural rearrangement in cytoplasmic 60S subunit maturation.

MATERIALS AND METHODS

Strains and genetic techniques. The strains used in this study are shown in Table 1. Strains MP001, MP002, MP004, MP006, MP011, and MP027 were obtained by homologous recombination (3, 28) in the wild-type strains BY4741/BY4742 (4). Strain MP010 was obtained by homologous recombination in MP001. Strains MP023, MP024, MP031, and MP086 were obtained by sporulating the diploids made by crossing MP002 and MP006, MP010 and MP011, MP001 and MP027, and YSC1178-7500470 and MP011, respectively. Strains MP099 and MP107 were obtained by sporulating the diploids made by crossing MP086 and YSC1021-552120. Strain DEH221+, described in Eisinger et al. (7), was provided by Bernard Trumpower (Dartmouth Medical School, Hanover, NH). Strain LMA374 was provided by Micheline Fromont-Racine (Institut Pasteur, Paris, France).

Minimal and glucose-based media were as described previously (23). Yeast strains were transformed using the lithium acetate method (21). All chemicals were obtained from Sigma (St. Louis, MO) unless noted.

Plasmids. pMP001 (*LEU2 CEN REI1*) and pMP002 (*LEU2 CEN REH1*) were made by PCR amplification of *REI1* or *REH1* (including ~300 nucleotides upstream and downstream, to include regulatory regions) from wild-type yeast genomic DNA with the *REI1* primers DMP001 (5′-GGGGGGGGATCCAGCACATCCACTCT CATTCCCGATATTCC) and DMP002 (5′-GGGGGGCTCGAGCTTCAGTCTT CAGCAGCTATTTCCTTTGCT) or the *REH1* primers DMP003 (5′-GGGGGG CTCGAGCCGTCCATGCGATATGAGCTGATTC) and DMP004 (5′-GGGGG GGTGTCCCAACCCCGTGTCCG). The PCR products were digested with BamHI and XhoI and ligated into the same sites of pRS315 (37). pMP003 (*LEU2 CEN 3×FLAG-REI1*) (where 3×FLAG indicates three copies of a FLAG tag) and pMP004 (*LEU2 CEN 3×FLAG-REH1*) were obtained by PCR mutagenesis of pMP001 and pMP002, respectively. pMP005 (*LEU2 CEN TEF*::*REH1*) was made by

* Corresponding author. Mailing address: Department of Biochemistry and Howard Hughes Medical Institute, University of Utah School of Medicine, 15 N Medical Drive East, Room 4800, Salt Lake City, UT 84112-5650. Phone for K. Mark Parnell: (801) 931-2420. Fax: (801) 746-5633. E-mail: markparnell1@gmail.com. Phone for Brenda L. Bass: (801) 581-4884. Fax: (801) 581-3824. E-mail: bbass@biochem.utah.edu.

▽ Published ahead of print on 11 May 2009.

TABLE 1. Yeast strains used in this study

Strain	Genotype	Reference or source
BY4741	*MAT***a** *his3Δ1 leu2Δ0 met15Δ0 ura3Δ0*	3
BY4742	*MATα his3Δ1 leu2Δ0 lys2Δ0 ura3Δ0*	3
YSC1178–7500470	*MAT***a** *his3Δ1 leu2Δ0 met15Δ0 ura3Δ0 LSG1-TAP*::*HIS3*	Open Biosystems
YSC1021–552120	*MAT***a** *his3Δ1 leu2Δ0 met15Δ0 ura3Δ0 rei1Δ*::*KanMX4*	Open Biosystems
MP001	*MAT***a** *his3Δ1 leu2Δ0 met15Δ0 ura3Δ0 rei1Δ*::*HIS3*	This study
MP004	*MAT***a** *his3Δ1 leu2Δ0 met15Δ0 ura3Δ0 arx1Δ*::*LEU2*	This study
MP002	*MATα his3Δ1 leu2Δ0 lys2Δ0 ura3Δ0 rei1Δ*::*HIS3*	This study
MP006	*MAT***a** *his3Δ1 leu2Δ0 met15Δ0 reh1Δ*::*URA3*	This study
MP010	*MAT***a** *his3Δ1 leu2Δ0 met15Δ0 arx1Δ*::*LEU2 rei1Δ*::*HIS3*	This study
MP011	*MATα his3Δ1 leu2Δ0 lys2Δ0 ura3Δ0 reh1Δ*::*URA3*	This study
MP023	*MAT***a** *his3Δ1 leu2Δ0 met15Δ0 ura3Δ0 reh1Δ*::*URA3 rei1Δ*::*HIS3*	This study
MP024	*MAT***a** *his3Δ1 leu2Δ0 ura3Δ0 arx1Δ*::*LEU2 reh1Δ*::*URA3 rei1Δ*::*HIS3*	This study
MP027	*MATα his3Δ1 leu2Δ0 met15Δ0 ura3Δ0 reh1Δ*::*LEU2*	This study
MP031	*MATα his3Δ1 leu2Δ0 lys2Δ0 ura3Δ0 reh1Δ*::*HIS3 rei1Δ*::*LEU2*	This study
MP086	*MATα his3Δ1 leu2Δ0 lys2Δ0 met15Δ0 ura3Δ0 LSG1-TAP*::*HIS3 reh1Δ*::*LEU2*	This study
MP099	*MAT***a** *his3Δ1 leu2Δ0 lys2Δ0 met15Δ0 ura3Δ0 LSG1-TAP*::*HIS3 rei1Δ*::*KanMX4*	This study
MP107	*MAT***a** *his3Δ1 leu2Δ0 lys2Δ0 met15Δ0 ura3Δ0 LSG1-TAP*::*HIS3 reh1Δ*::*LEU2 rei1Δ*::*KanMX4*	This study
DEH221+	*MATα rpl10Δ*::*HIS3* pDEQ2 [*CEN URA3 GAL1-10*$_{UAS}$::*RPL10*]	8
LMA374	*MATα his3Δ1 leu2Δ0 lys2Δ0 met15Δ0 ura3Δ0 rpl24aΔ*::*NAT rpl24bΔ*::*HYGRO*	M. Fromont Racine

PCR amplification of the *REH1* open reading frame using primers DMP005 (5′-GGGGGGGGATCCATGAGCTCTACTTTCTTTACATGCAACTG) and DMP006 (5′-GGGGGGCTCGAGCTATTGCAACAACTCATCCCTGTA ATGTG). The PCR products were digested with BamHI and XhoI and ligated into the same sites of p415 TEF (31). pAJ1004 (*URA3 CEN TIF6-GFP*) (GFP is green fluorescent protein) and pAJ1015 (*URA3 CEN ARX1-GFP*) (19) were provided by Arlen Johnson (University of Texas, Austin, TX).

Sucrose gradients. Sucrose density sedimentation was performed essentially as described previously (9) with modifications as noted. For polysome profiles in the presence of low salt, approximately 1 liter of yeast was grown at 30°C in rich medium to mid-log phase (0.7 to 1.0 optical density at 600 nm [OD_{600}] units). Cycloheximide (100 μg/ml final concentration) was added to the culture, followed immediately by chilling on ice and pelleting of cells by centrifugation at 4°C (3,000 × *g* for 5 min). Cells were washed in ice-cold breaking buffer A (20 mM Tris · HCl, pH 7.5, 100 mM NaCl, 30 mM $MgCl_2$, 100 μg/ml cycloheximide, 200 μg/ml heparin), repelleted by centrifugation as above, resuspended in breaking buffer A (~1.5 ml per g of wet cell weight), lysed by glass bead vortexing (10 cycles of 45 s of vortexing followed by 45 s on ice), and cleared by centrifugation (20,000 × *g* at 4°C for 20 min). Approximately 10 OD_{260} units of cleared lysate were layered on 11 ml of 7 to 47% (mass/vol) sucrose gradients (containing 50 mM Tris · HCl, pH 7.5, 50 mM KCl, 12 mM $MgCl_2$, 1 mM dithiothreitol [DTT]) and centrifuged in an SW41 Ti rotor, Optima L-90K Ultracentrifuge (Beckman Coulter Inc., Fullerton, CA) at 40,000 rpm (200,000 × *g*) and 4°C for 3 h. The fractions were scanned at 254 nm and fractionated in an ISCO gradient collector (Teledyne Isco Inc., Lincoln, NE).

For runoff sucrose density sedimentation, extracts were made with breaking buffer A in the absence of cycloheximide. Ultracentrifugation through 11 ml of 10 to 40% (mass/vol) sucrose gradients, containing breaking buffer A without cycloheximide, was performed at 40,000 rpm and 4°C for 4 h.

For subunit stoichiometry determination in the absence of Mg^{2+}, cell cultures grown as detailed above were lysed in breaking buffer B (50 mM Tris · HCl, pH 7.5, 50 mM NaCl, 1 mM DTT), and separated by ultracentrifugation on 11 ml of 15 to 30% (mass/vol) sucrose gradients (made with buffers containing 50 mM Tris · HCl, pH 7.5, 50 mM KCl, 1 mM DTT) at 40,000 rpm and 4°C for 6 h. Ratios of 40S and 60S subunits were calculated by determining the areas under the respective A_{254} traces. For subunit stoichiometry determination in the presence of high salt, lysates were made in breaking buffer C (50 mM Tris · HCl, pH 7.5, 800 mM KCl, 10 mM $MgCl_2$, 1 mM DTT), and separated by ultracentrifugation on 11 ml of 10 to 40% (mass/vol) sucrose gradients made with breaking buffer C at 40,000 rpm and 4°C for 4 h. Ratios of 40S and 60S subunits were calculated as with experiments lacking Mg^{2+}.

Immunoprecipitation of FLAG fusion proteins. Cells expressing either 3×FLAG-Rei1 (MP002 harboring plasmid pMP003 [MP002/pMP003]) or 3×FLAG-Reh1 (MP011/pMP004) were grown in the appropriate synthetic medium to ~1 OD_{600} unit, lysed by glass bead vortexing, and cleared as described above. Immunoprecipitation in the presence of 150 mM NaCl using anti-FLAG M2 Affinity Gel (Sigma, St. Louis, MO) was according to the manufacturer's protocol. Immunoprecipitated complexes were separated by 5 to 15% gradient polyacrylamide-sodium dodecyl sulfate (SDS) gel electrophoresis (Ready Gel; Bio-Rad, Hercules, CA), followed by staining with Coomassie blue or Western blotting. Proteins from gel slices were identified by proteolysis/mass spectrometry using the Mascot search engine (Matrix Science, Inc., Boston, MA); mass spectrometry was performed by the Mass Spectrometry Core Facility at the University of Utah Medical School (Salt Lake City, UT).

Western blotting. Sucrose gradient fraction proteins were precipitated with 57% acetone overnight at −20°C, pelleted by centrifugation (20,000 × *g* at 4°C for 30 min), separated on 5 to 15% polyacrylamide-SDS gels as described above, and transferred to nitrocellulose membranes (Immobilon-P; Millipore, Billerica, MA). The following primary antibodies were used in this study at the indicated dilutions in 3% nonfat milk-TTBS (20 mM Tris, pH 7.5, 150 mM NaCl, 0.1% Tween 20): mouse monoclonal antibodies anti-FLAG M2 (1:10,000; Sigma, St. Louis, MO) and anti-Rpl3 (1:5,000; J. Warner, Albert Einstein College of Medicine, New York, NY); and rabbit polyclonal antibodies anti-Arx1 (1:1,000; M. Fromont-Racine, Institut Pasteur, Paris, France), anti-Nmd3 (1:5,000; A. Johnson, University of Texas, Austin, TX), anti-Rei1 (1:1,000, M. Fromont-Racine), anti-Rlp24 (1:1,000, M. Fromont-Racine), anti-Rpl10 (1:2,000, B. Trumpower, Dartmouth Medical School, Hanover, NH), and anti-Tif6 (1:1,000, F. Fasiolo, IBMC, Strasbourg, France). Secondary antibodies (goat anti-mouse and goat anti-rabbit antibody–horseradish peroxidase conjugates) were used at 1:20,000 dilutions, and visualization of peroxidase activity was performed with a SuperSignal West Femto chemiluminescence kit (Pierce, Rockford, IL).

[^{35}S]methionine pulse-chase analysis. Pulse-chase analysis of 3×FLAG-Reh1 or 3×FLAG-Rei1 immunoprecipitations was performed essentially as described previously (15). 3×FLAG-Reh1 (MP011/pMP004) or 3×FLAG-Reh1 (MP002/pMP003) strains were grown in 250 ml of minimal medium lacking leucine and methionine at 30°C to mid-log phase (OD_{600} of ~1). Cells were pelleted and resuspended in 9 ml of the same medium. L-[^{35}S]methionine (3.5 mCi EXPRE^{35}S^{35}S protein labeling mix; Perkin Elmer, Waltham, MA) was then added. After 5 min, cells were pelleted and resuspended in 9 ml of medium containing 200 μg/ml unlabeled methionine. Samples (1.0 ml) were removed to an ice bath upon addition of unlabeled methionine (0 min), and at 5, 10, 20, and 40 min after chase. Pelleted cells were lysed by glass bead vortexing on ice and cleared, and FLAG immunoprecipitation was carried out as described above. Immunoprecipitated proteins were separated by SDS gel electrophoresis and transferred to nitrocellulose, and Rpl3 was visualized by Western blotting (as described above). [^{35}S]methionine was subsequently visualized by autoradiography.

Fluorescence microscopy. Cells were transformed with a centromeric plasmid expressing either *ARX1-GFP* (pAJ1015) or *TIF6-GFP* (pAJ1004). To determine localization of Arx1-GFP in the *rei1*Δ strain upon Reh1 overexpression, the MP002 strain was transformed with pAJ1015 and pMP005 simultaneously. Cells were cultured at either 23°C for 16 h or 37°C for 8 h and mounted in liquid minimal culture medium on glass slides. The images were taken at room temperature on an Axioscop 2 microscope (Carl Zeiss Inc., Thornwood, NY) equipped with 100× oil immersion objective lenses (numerical aperture, 1.30 to 0.60) and a Retiga 2000R digital camera

(QImaging, Pleasonton, CA) and analyzed using Microsuite Five software (Olympus Imagine America, Inc., Center Valley, PA).

RESULTS

Reh1 is associated with newly synthesized 60S subunits and biogenesis factors. To determine whether the overlapping functions of Reh1 and Rei1 involve 60S subunit biogenesis, we first asked whether Reh1, like Rei1, associates with free 60S subunits. As a means of probing for Reh1 and Rei1 and to facilitate coimmunoprecipitation experiments, we created yeast strains wherein native Reh1 or Rei1 was replaced with N-terminally tagged 3×FLAG-Reh1 or 3×FLAG-Rei1, respectively. Genetic rescue experiments indicated that the N-terminal tag did not affect the function of either protein (our unpublished data). When cycloheximide-treated extracts were separated by sucrose density ultracentrifugation, we found that Reh1 and Rei1 cosedimented primarily with free 60S subunits (Fig. 1A). This result indicated that Reh1 associates with pre-60S particles that have not yet entered the translating pool, as do many other 60S subunit biogenesis factors including Rei1 (19, 27).

To rule out the possibility that Reh1 acts on mature rather than newly synthesized free 60S subunits, we utilized a combination of pulse-chase ^{35}S labeling and immunoprecipitation (15, 24). Rapidly growing cells expressing either 3×FLAG-Reh1 or 3×FLAG-Rei1 were pulse-labeled (5 min) with L-[^{35}S]methionine, followed by a chase with excess unlabeled methionine. FLAG immunoprecipitations were performed on cells removed at various time points, and ^{35}S specific activity of 60S subunit r-proteins was analyzed (Fig. 1B). We observed that the specific activity of 60S r-proteins, but not a FLAG-interacting nonspecific protein (^{35}S control), decreased rapidly as a function of time after chase for both Reh1 and Rei1 immunoprecipitations. The amount of immunoprecipitated Rlp3, monitored by Western blotting, remained unchanged throughout the time course. This result indicated that both Reh1 and Rei1 associate primarily with nascent pre-60S particles, followed by their release from mature 60S subunits. Our findings are similar to previous pulse-chase analyses of 60S biogenesis factors (15, 24).

We next used immunoprecipitation of 3×FLAG-Reh1 or 3×FLAG-Rei1 to identify the cytoplasmic biogenesis factors that associate with Reh1- or Rei1-bound pre-60S particles. Coimmunoprecipitating proteins were separated by polyacrylamide gel electrophoresis and identified either by Coomassie staining and subsequent mass spectrometry analysis or by Western blotting (Fig. 1C). Several biogenesis factors that are known to be present on cytoplasmic pre-60S particles coprecipitated with Reh1 as well as Rei1. Lsg1 (12, 24) was pulled down in near-stoichiometric amounts with Reh1 and Rei1, as indicated by Coomassie staining, and identified by mass spectrometry. In addition, Western blotting demonstrated similar levels of Nmd3 (14, 16) and Tif6 (2) pulled down by Reh1 and Rei1. The coimmunoprecipitation of Reh1 with known cytoplasmic and nucleo-cytoplasmic pre-60S biogenesis factors strongly suggested that Reh1, like Rei1, acts on the cytoplasmic pre-60S particle.

Rei1, but not Reh1, associates with Arx1-bound pre-60S particles. Despite similarities between the biogenesis factors coimmunoprecipitated with Reh1 and Rei1, there were notable differences. First, Reh1 failed to pull down Rei1, as con-

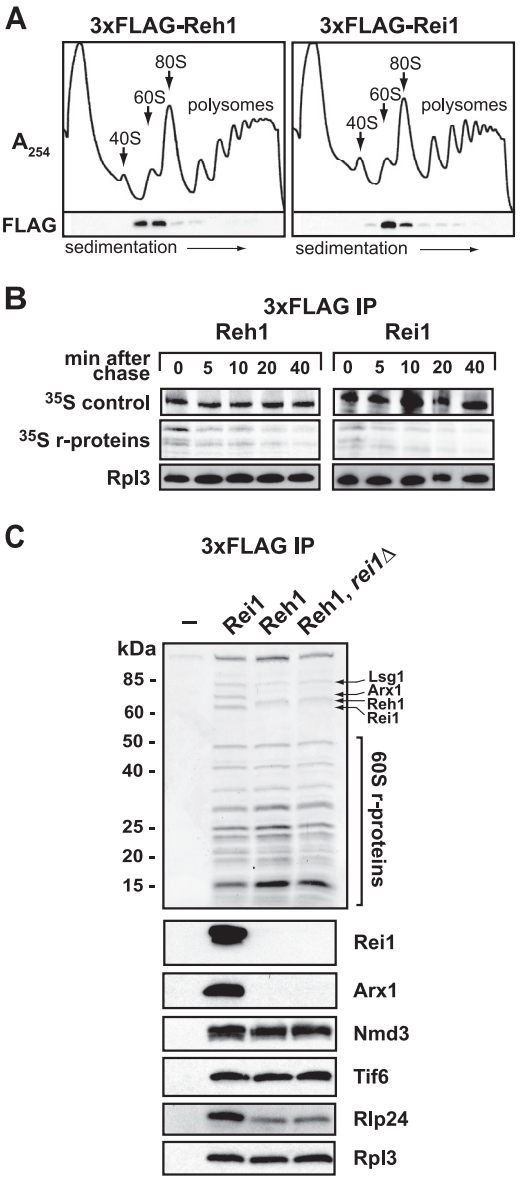

FIG. 1. Reh1 associates with free nascent 60S subunits and 60S biogenesis factors but does not associate with Arx1. (A) Cycloheximide-treated extracts from *reh1*Δ *3×FLAG-REH1* (MP011/pMP004) or *rei1*Δ *3×FLAG-REI1* (MP002/pMP003) cells were separated by sucrose density sedimentation (7% to 47% sucrose). Positions of 40S, 60S, and 80S subunits are indicated. 3×FLAG-Rei1 or 3×FLAG-Reh1 was detected by Western blotting using anti-FLAG antibody. (B) Nascent subunits chase through Reh1 and Rei1 complexes. Cells containing 3×FLAG-Rei1 or 3×FLAG-Reh1 were labeled for 5 min with [^{35}S]methionine, followed by addition of excess unlabeled methionine as described in Materials and Methods. Samples were removed at the times indicated after addition of chase. Extracts were prepared, and proteins were immunoprecipitated with anti-FLAG antibody. Immunoprecipitated proteins were analyzed by Western blotting for Rpl3 (anti-Rpl3) and visualized by autoradiography ([^{35}S]Met). (C) Wild-type (−), *rei1*Δ *3×FLAG-REI1* (Rei1), *reh1*Δ *3×FLAG-REH1* (Reh1), and *reh1*Δ *rei1*Δ *3×FLAG-REH1* (Reh1, *rei1*Δ) lysates were immunoprecipitated with anti-FLAG antibody, and the resulting proteins were separated by SDS-polyacrylamide gel electrophoresis and stained with Coomassie brilliant blue. Gel bands indicated by arrows were excised from each lane and treated with trypsin, and the protein fragments were identified by mass spectrometry. Western blotting of immunoprecipitated proteins with the indicated primary antibodies was as described in Materials and Methods. IP, immunoprecipitation.

firmed by Western blotting. Likewise, Coomassie staining and mass spectrometry analysis indicated that Rei1 also failed to pull down Reh1. This finding indicated that Reh1 and Rei1 do not act simultaneously on the same pre-60S particle. Given the high degree of sequence similarity, it is possible that Reh1 and Rei1 share a partially overlapping pre-60S subunit binding site that precludes simultaneous binding.

A second difference between Reh1 and Rei1 immunoprecipitations was that Reh1 failed to pull down Arx1, as confirmed by Western blotting. This finding suggested one of two possibilities: (i) Reh1 binds to pre-60S subunits downstream of Rei1 binding and Rei1/Arx1 dissociation, or (ii) Reh1 binds to a subset of pre-60S particles that do not contain Arx1. We observed higher levels of Rlp24, a biogenesis factor that binds to the pre-60S particle in the nucleolus and is dissociated shortly after cytoplasmic export (32, 34), in the Rei1 immunoprecipitation (Fig. 1C). One interpretation of this result is that Rei1 binds to pre-60S particles prior to Reh1. However, previous studies show that the vast majority of Rlp24 dissociates from the cytoplasmic pre-60S subunit prior to Rei1 binding (27). If Rei1 and Reh1 are both binding to pre-60S subunits that are rapidly losing Rlp24, the small difference we observe in Rlp24 levels may not be meaningful.

Given the possibility that Rei1 and Reh1 compete for binding to the pre-60S particle, we wished to determine whether deletion of *REI1* affected Reh1 binding. We found no difference between Reh1 immunoprecipitations in the wild-type and *rei1*Δ strains (Fig. 1C), indicating that the specificity and kinetics of Reh1 binding are independent of Rei1.

The overlapping functions of Rei1 and Reh1 are independent of Arx1 recycling. Our immunoprecipitation data suggested that Reh1 binds to and acts on pre-60S subunits lacking Arx1, whereas Rei1 interacts with Arx1-bound 60S subunits. This finding led us to consider the possibility that Reh1 acts redundantly with Rei1 in promoting a step in the cytoplasmic 60S maturation pathway distinct from Arx1 recycling.

It was previously shown that the cold-sensitive *rei1*Δ growth phenotype was due to the effects of mislocalized Arx1; when *ARX1* was deleted in the *rei1*Δ background, the growth phenotype was rescued to wild-type levels (19, 27). If the overlapping function of Reh1 and Rei1 is distinct from Arx1 nuclear reimport, we reasoned that the presence of Reh1 would be critical in both *rei1*Δ and *arx1*Δ *rei1*Δ strains. Indeed, we observed that deletion of *REH1* in either the *rei1*Δ background (*reh1*Δ *rei1*Δ) or *arx1*Δ *rei1*Δ background (*arx1*Δ *reh1*Δ *rei1*Δ) resulted in an extremely slow growth phenotype (Fig. 2A). This result confirmed our hypothesis that the overlapping functions of Reh1 and Rei1 are independent of Arx1 recycling.

Our genetic analysis suggested an Arx1-independent function for Reh1. However, since overexpression of Reh1 partially rescues the *rei1*Δ growth phenotype (22, 27), we performed additional analyses designed to reveal Arx1-dependent functions for Reh1. We did not observe a genetic interaction between *ARX1* and *REH1* (Fig. 2A, *arx1*Δ *reh1*Δ), nor did deletion of *REH1* affect Arx1-GFP localization in either wild-type or *rei1*Δ backgrounds (Fig. 2B). However, we found that overexpression of Reh1 in the *rei1*Δ background resulted in the rescue of Arx1-GFP nuclear localization (Fig. 2C), a result also observed by others (C. Savaneu and M. Fromont-Racine, personal communication). Interestingly, the ability of Arx1 to cosediment with free 60S subunits, which was previously shown to be absent in the *rei1*Δ strain (27), was not rescued by overexpressing Reh1 in the *rei1*Δ background (Fig. 2D), a result also observed by others (26). We concluded that under normal cellular conditions, Reh1 does not influence Arx1 recycling. When overexpressed, Reh1 appears to promote the nuclear reimport of Arx1 but cannot render Arx1 capable of binding to pre-60S subunits and, presumably, participating in the ribosome biogenesis pathway.

While studying the functional overlap between Arx1 and Reh1, we also uncovered a novel feature of the functional overlap between Arx1 and Rei1. We found that while the growth defects of the *rei1*Δ strain were alleviated when cells were grown at 37°C (Fig. 2A), as previously observed (19, 22, 27), the location of Arx1-GFP continued to be predominantly cytoplasmic when grown at the higher temperature (Fig. 2B). This finding indicated that mislocalized, cytoplasmic Arx1 does not lead to growth defects at high temperatures.

We considered the possibility that the overlapping functions of Reh1 and Rei1 influence Tif6 recycling, based on previous evidence that *REI1* deletion changes Tif6 localization from primarily nuclear to cytoplasmic (27). However, in our hands Tif6-GFP localization remained primarily nuclear in *rei1*Δ as well as in *reh1*Δ *rei1*Δ cells (Fig. 2E). We also considered the possibility that the association of *trans*-acting factors Lsg1, Nmd3, and Tif6 with pre-60S particles might be disrupted in the absence of Reh1 and Rei1. However, we observed that cosedimentation of Lsg1, Nmd3, and Tif6 with free 60S subunits was the same in wild-type, *rei1*Δ, and *reh1*Δ *rei1*Δ strains (Fig. 2F). We concluded that it was unlikely that the overlapping functions of Reh1 and Rei1 are critical for the recycling/association/dissociation of a known cytoplasmic *trans*-acting factor.

The overlapping functions of Reh1 and Rei1 are important for polysome formation and 40S-60S subunit joining. To better understand the overlapping functions of Reh1 and Rei1 in 60S subunit maturation, we obtained polysome profiles for strains lacking both Reh1 and Rei1 (Fig. 3A). The wild-type and *reh1*Δ polysome profiles were indistinguishable. The *reh1*Δ *rei1*Δ and *arx1*Δ *reh1*Δ *rei1*Δ polysome profiles, like the previously described *rei1*Δ profile (19, 27), were distinguished by half-mers: peaks sedimenting slightly faster than monosome, disome, and trisome peaks and thought to indicate defects in 60S subunit biogenesis or the 60S subunit joining step of translation initiation (17). We also observed diminished 80S peaks and polysome levels in the *reh1*Δ *rei1*Δ and *arx1*Δ *reh1*Δ *rei1*Δ strains. These findings suggested that translation initiation may be diminished in cells lacking both Reh1 and Rei1, possibly due to defects in subunit joining.

To verify that cells lacking both Reh1 and Rei1 are defective in subunit joining, we monitored the formation of 80S couples (monomers formed in the absence of mRNA) in cell extracts prepared in the absence of cycloheximide to allow translation runoff (Fig. 3B). We found that 80S couples readily formed in wild-type and *reh1*Δ extracts, with very few observable free 40S subunits (the free 60S subunits are obscured by the large 80S peak). In contrast, the *rei1*Δ strain demonstrated an increase in the 40S peak and a corresponding decrease in the 80S peak that were indicative of a subunit joining defect. The free 40S peak was considerably larger, and the 80S peak was considerably smaller in *reh1*Δ *rei1*Δ and *arx1*Δ *reh1*Δ *rei1*Δ strains,

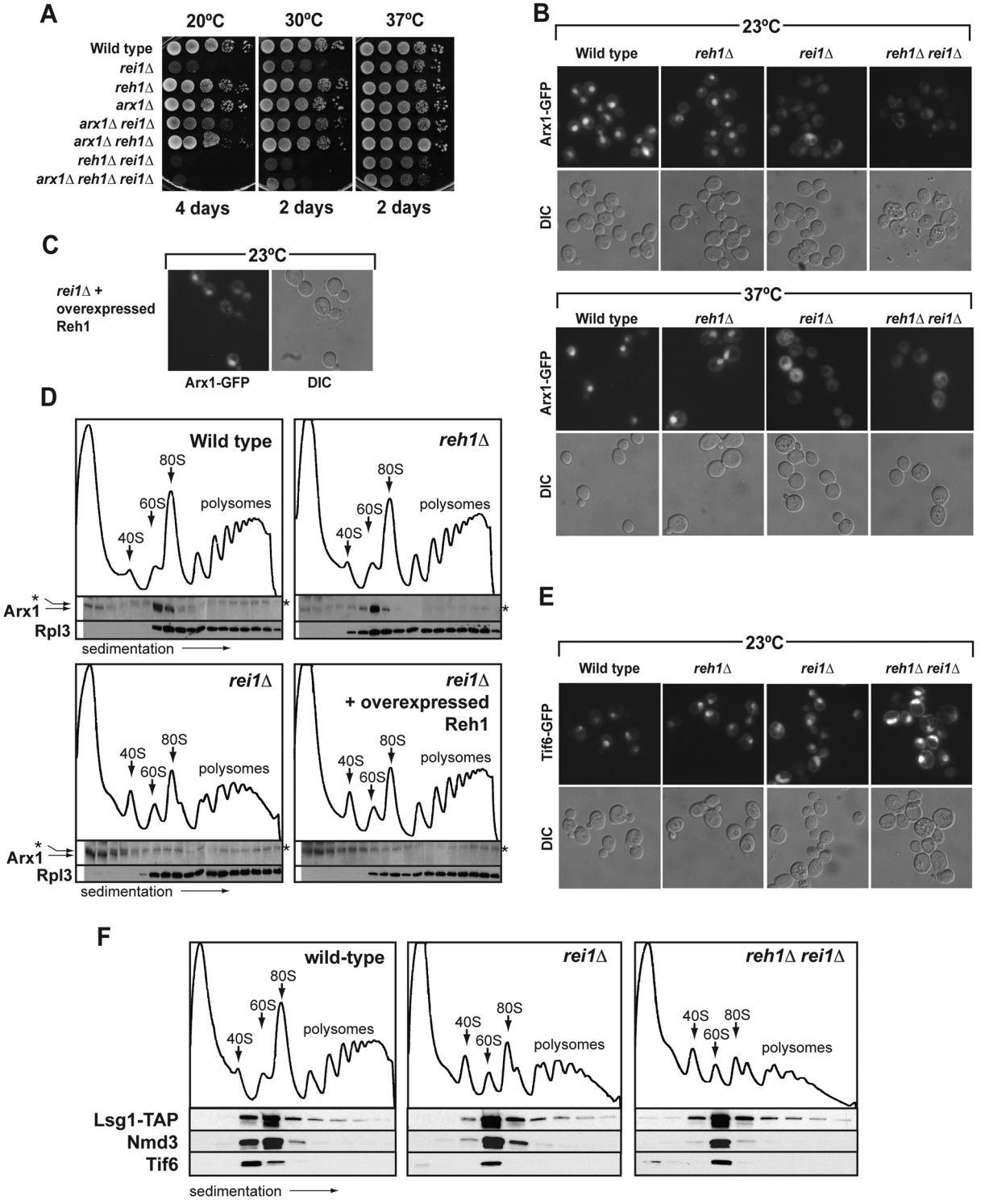

FIG. 2. Analysis of the functional relationship between Reh1/Rei1 and *trans*-acting factors. (A) The overlapping functions of Reh1 and Rei1 are independent of Arx1 recycling. Tenfold serial dilutions of yeast cells with indicated genotypes were spotted onto rich medium plates and incubated at the indicated temperature for the indicated period. The following strains were used: wild type, BY4742; *reh1*Δ, MP011; *rei1*Δ, MP002; *arx1*Δ, MP004; *arx1*Δ *rei1*Δ, MP010; *reh1*Δ *rei1*Δ, MP023; and *arx1*Δ *reh1*Δ *rei1*Δ, MP024. (B) Fluorescence microscopy analysis of Arx1-GFP localization was performed in the wild-type (BY4742), *reh1*Δ (MP027), *rei1*Δ (MP002), and *reh1*Δ *rei1*Δ (MP031) strains grown overnight at 23°C or for 8 h at 37°C, as indicated. (C) Fluorescence microscopy analysis of Arx1-GFP localization in the *rei1*Δ (MP002) strain, in which Reh1 is overexpressed (from plasmid pMP003). Cells were grown overnight at 23°C. (D) Cosedimentation of Arx1 with free subunits. Polysome profiles (7% to 47% sucrose) of cycloheximide-treated extracts from the indicated strains: wild-type (BY4741), *reh1*Δ (MP006), *rei1*Δ (MP001), or *rei1*Δ *TEF*::*REH1* (MP001/pMP005). Fractions were probed for the presence of Arx1 and Rpl3 by Western blotting. The asterisk denotes a nonspecific band in Arx1 Western blots. (E) Tif6 localization is primarily nuclear in cells lacking both Reh1 and Rei1. Fluorescence microscopy analysis of Tif6-GFP localization in the indicated strains, grown overnight at 23°C. (F) The association of *trans*-acting biogenesis factors with 60S subunits is not affected upon deletion of both *REH1* and *REI1*. Polysome profiles (7% to 47%) are shown for the indicated, cycloheximide-treated strains: wild-type (YSC1178-7500470), *rei1*Δ (MP099), and *reh1*Δ *rei1*Δ (MP107). Fractions were probed for Lsg1-TAP, Nmd3, and Tif6 by Western blotting. DIC, differential interference contrast image.

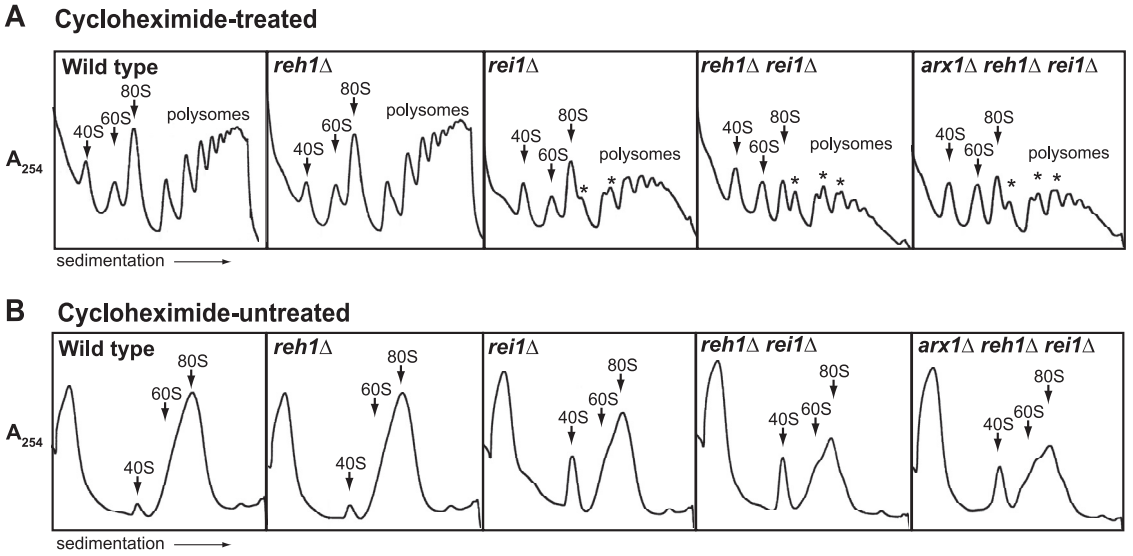

FIG. 3. Polysome levels and subunit joining are defective in cells lacking both Reh1 and Rei1. (A) Polysome profiles (7% to 47% sucrose) of cycloheximide-treated wild-type (BY4742), *reh1*Δ (MP011), *rei1*Δ (MP002), *reh1*Δ *rei1*Δ (MP023), and *arx1*Δ *reh1*Δ *rei1*Δ (MP024) strains grown in rich medium at 30°C. Asterisks denote the presence of half-mers (see text for details). (B) Sucrose density sedimentation (10% to 40% sucrose) of the same strains under conditions of runoff translation.

suggesting that subunit joining was particularly defective in the absence of both Reh1 and Rei1. Our findings were consistent with two possibilities: cells lacking both Reh1 and Rei1 either produce dramatically substoichiometric amounts of 60S subunits or assemble 60S subunits that bind poorly to 40S subunits.

60S subunit salt stability is dramatically affected in strains lacking both Reh1 and Rei1. To address 60S/40S stoichiometry, we first used buffer lacking Mg^{2+} to resolve 40S and 60S subunits by sucrose density ultracentrifugation (13) and compared the relative levels of 40S and 60S subunits by calculating the areas beneath the respective A_{254} traces (Fig. 4A). In wild-type and *reh1*Δ strains, the 60S/40S ratios were near 2.0, as previously reported for wild-type cells (36). The 60S/40S ratio in *rei1*Δ cells was 1.77, which was significant though less dramatic than the previously measured value of 1.36 (30), possibly due to differences in growth temperature of cold-sensitive *rei1*Δ (23°C in the study of Meyer et al. [30] versus 30°C here). Interestingly, although *reh1*Δ *rei1*Δ and *arx1*Δ *reh1*Δ *rei1*Δ strains demonstrated dramatically slow growth (Fig. 2A) and

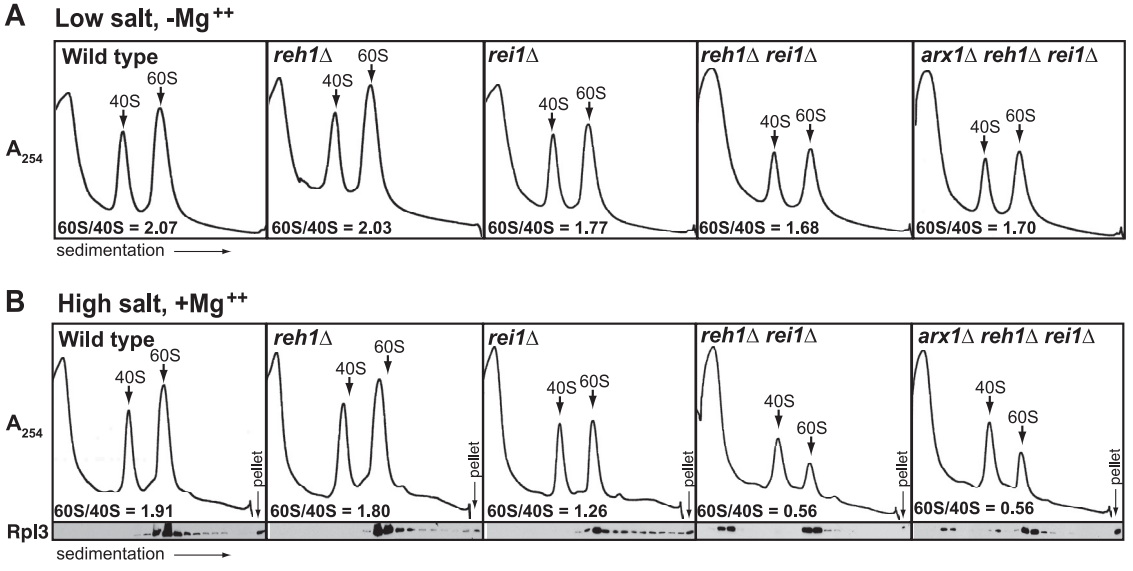

FIG. 4. Cells lacking both Reh1 and Rei1 demonstrate modest subunit stoichiometry and dramatic 60S salt lability phenotypes. Extracts were prepared from wild-type (BY4742), *reh1*Δ (MP011), *rei1*Δ (MP002), *reh1*Δ *rei1*Δ (MP023), and *arx1*Δ *reh1*Δ *rei1*Δ (MP024) strains and fractionated by sucrose density sedimentation (15% to 30% sucrose) in the absence of Mg^{2+} (A) or in the presence of high salt concentrations (B). Subunit ratios were determined by calculating the area under the A_{254} trace for each respective peak. Fractions were also probed for the presence of 60S subunit r-protein Rpl3 by Western blotting.

impaired polysome profiles (Fig. 3A) relative to *rei1*Δ at 30°C, we did not observe a further decrease in the 60S/40S ratios in strains lacking both Reh1 and Rei1. The most noticeable difference between *rei1*Δ and *reh1*Δ *rei1*Δ strains was a reduction in the levels of both ribosomal subunits relative to the A_{254} peak at the top of the sucrose gradient, suggesting that the total ribosome concentration may be diminished in these strains. Our results indicated that the observed defects in polysome formation and subunit joining were not simply due to substoichiometric 60S subunit levels.

When we utilized high-salt conditions (800 mM KCl plus 10 mM $MgCl_2$) rather than an absence of Mg^{2+} to separate 40S and 60S subunits (38, 39), we observed a strikingly different result (Fig. 4B). The 60S/40S ratios from wild-type and *reh1*Δ strains were relatively unchanged under high-salt conditions, but *rei1*Δ and especially *reh1*Δ *rei1*Δ and *arx1*Δ *reh1*Δ *rei1*Δ strains showed a dramatic decrease in 60S subunits. Our analysis indicated that ~70% of 60S particles are salt labile in cells lacking both Reh1 and Rei1. When the high-salt sucrose gradient fractions were probed for the presence of 60S subunit r-protein Rpl3, we found a significant amount of Rpl3 near the top of the *reh1*Δ *rei1*Δ and *arx1*Δ *reh1*Δ *rei1*Δ gradients but not those from wild-type, *reh1*Δ, or *rei1*Δ cells (Fig. 4B). We surmised that 60S subunits from cells lacking both Reh1 and Rei1 fall apart in the presence of high salt.

We considered the possibility that one or more r-proteins are not loaded onto 60S subunits in the *reh1*Δ *rei1*Δ strain, leading to salt instability. We determined the r-protein composition of wild-type and *reh1*Δ *rei1*Δ 60S subunits (Fig. 4A) by proteolysis/mass spectrometry and did not observe any differences between strains (Table 2). Nor did we observe differences in rRNA composition profiles between wild-type and *reh1*Δ *rei1*Δ 60S subunits (our unpublished data). Thus, 60S subunit salt instability in the *reh1*Δ *rei1*Δ strain likely stems from defects in conformation rather than r-protein or rRNA composition.

Salt-unstable 60S subunits are also observed in cells depleted of Rpl10 and, to a lesser extent, in *rpl24*ΔΔ cells. We wondered if the defects in 60S subunit stability observed in the *reh1*Δ *rei1*Δ strain are present in other strains wherein cytoplasmic 60S subunit maturation is affected. To address this issue, we investigated the salt stability of 60S subunits from strains lacking one of two distinct, cytoplasmically loaded r-proteins: Rpl24 and Rpl10. Rpl24 is a nonessential r-protein (1) that may affect the kinetics of translation (6). Rpl10, in contrast, is essential (41) and necessary for 40S-60S subunit joining (7). Using a yeast strain wherein both copies of *RPL24* were deleted (*rpl24*ΔΔ), we observed a decrease in polysome levels (Fig. 5A) similar to that observed previously (26). Though subunit stoichiometry was not affected in the *rpl24*ΔΔ strain, we observed that ~25% of 60S subunits appeared to be salt labile (Fig. 5A). Rpl10-depleted cells demonstrated greatly reduced polysomes levels, a significant (~25%) decrease in 60S subunits relative to 40S subunits along with a large overall decrease in ribosomes, and a very large fraction (~70%) of salt-labile 60S subunits (Fig. 5B). The similarity in 60S subunit salt lability between Rpl10-depleted and *reh1*Δ *rei1*Δ cells led us to consider the possibility that deletion of *REH1* and *REI1* might affect Rpl10 loading. Mass spectrometry data showed that Rpl10 is present on *reh1*Δ *rei1*Δ 60S subunits (Table 2) but did not indicate levels relative to wild-type 60S subunits. When Rpl10 levels of free 60S subunits from *reh1*Δ *rei1*Δ, *arx1*Δ *reh1*Δ *rei1*Δ, Rpl10-undepleted, and Rpl10-depleted cells were compared by Western blotting (Fig. 5C), we found no defect in Rpl10 in cells lacking both Reh1 and Rei1, indicating that Rpl10 loading does not involve Reh1/Rei1. We concluded that cytoplasmic loading of r-proteins, as well as the overlapping functions of Reh1/Rei1, affects 60S subunit stability.

TABLE 2. 60S subunit mass spectrometry results

No. of matching peptides identified[a]	Wild-type protein(s)	*reh1*Δ *rei1*Δ protein(s)[b]
>3	Rpl1A/B	Rpl1A/B
	Rpl2A/B	Rpl2A/B
	Rpl3	Rpl3
	Rpl4A/B	Rpl4A/B
	Rpl5	Rpl5
	Rpl6A/B	Rpl6A/B
	Rpl7A/B	Rpl7A/B
	Rpl8A/B	Rpl8A/B
	Rpl9A/B	Rpl9A/B
	Rpl10	Rpl10
	Rpl11A/B	Rpl11A/B
	Rpl12A/B	Rpl12A/B
	Rpl13A/B	Rpl13A/B
	Rpl14A/B	Rpl14A/B
	Rpl15A/B	Rpl15A/B
	Rpl16A/B	Rpl16A/B
	Rpl17A/B	Rpl17A/B
	Rpl18A/B	Rpl18A/B
	Rpl19A/B	Rpl19A/B
	Rpl20A/B	Rpl20A/B
	Rpl21A/B	Rpl21A/B
	Rpl22A/B	Rpl22A/B
	Rpl23A/B	Rpl23A/B
	Rpl24A/B	Rpl24A/B
	Rpl25	Rpl25
	Rpl26A/B	Rpl26A/B
	Rpl27A/B	Rpl27A/B
	Rpl28	Rpl28
	Rpl30	Rpl30
	Rpl31A/B	Rpl31A/B
	Rpl32	Rpl32
	Rpl33A/B	Rpl33A/B
	Rpl35A/B	Rpl35A/B
	Rpl36A/B	Rpl36A/B
	Rpl38	Rpl38
	Rpl42A/B	Rpl42A/B
	Rpp0	Rpp0
1–3	Rpl29	Rpl29
	Rpl34A/B	Rpl34A/B
	Rpl37A/B	Rpl37A/B
	Rpl39	Rpl39
	Rpl40A/B	Rpl40A/B
0	Rpl41A/B	Rpl41A/B

[a] Results of two independent experiments. Values are numbers of peptides identified by mass spectrometry that corresponded to a particular ribosomal protein.
[b] Strain MP023.

DISCUSSION

Here, we have investigated the overlapping functions of Reh1 and Rei1 in budding yeast. We found that Reh1, like Rei1, is a cytoplasmic 60S subunit biogenesis factor. Reh1

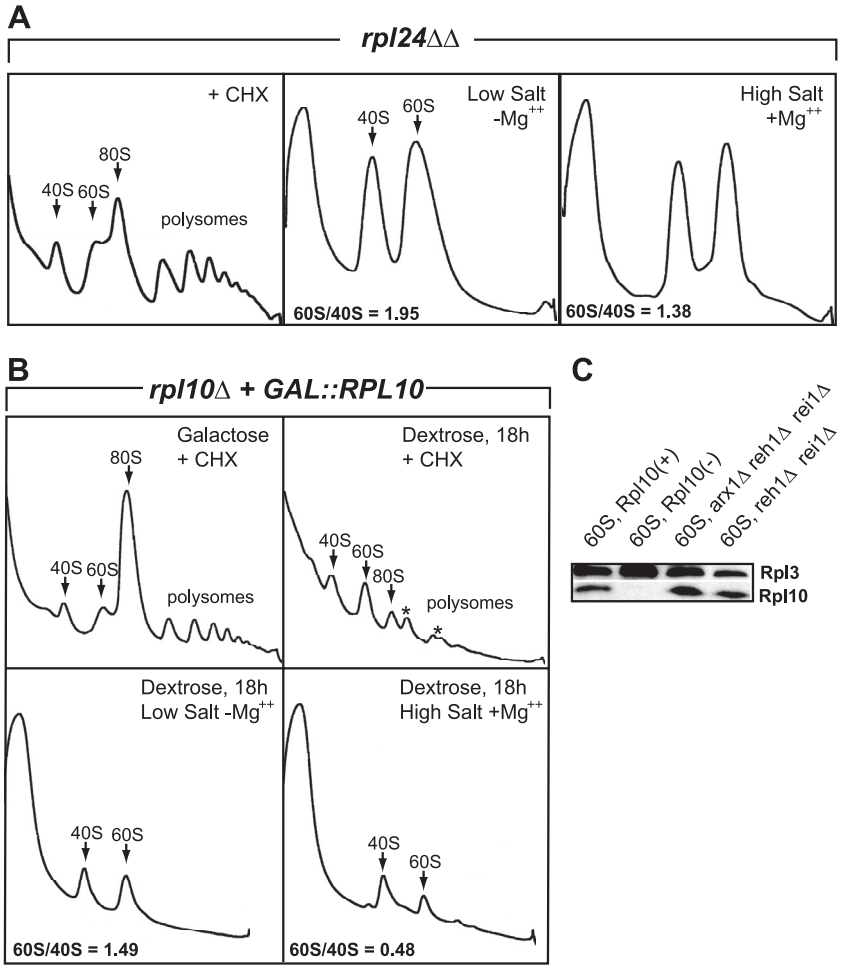

FIG. 5. Salt-unstable 60S subunits are found in Rpl10-depleted and, to a lesser degree, *rpl24*ΔΔ cells. (A) Analysis of the *rpl24*ΔΔ strain (LMA374) grown at 30°C: polysome profile (7% to 47% sucrose) of cycloheximide (CHX)-treated extracts (left panel); subunit stoichiometry determined by sucrose density sedimentation (10% to 40% sucrose) in the absence of Mg^{2+} (middle panel); salt lability of 60S subunits determined by sucrose density sedimentation (10% to 40% sucrose) in high salt (800 mM KCl and 10 mM Mg^{2+}) (right panel). (B) Analysis of the Rpl10-depletion strain (DEH221+), grown in dextrose or galactose as indicated, at 30°C. The polysome profiles (7% to 47% sucrose) of cycloheximide-treated extracts grown on galactose [Rpl10(+)] (and on dextrose for 18 h [Rpl10(])] are shown in the top panels. Subunit stoichiometry of cells grown on dextrose for 18 h [Rpl10(−)], determined by sucrose density sedimentation (10% to 40% sucrose) in the absence of Mg^{2+} is shown in the lower left panel. Salt lability of 60S subunits from cells grown on dextrose for 18 h [Rpl10(−)], determined by sucrose density sedimentation (10% to 40% sucrose) in high salt (800 mM KCl, 10 mM Mg^{2+}) is shown in the lower right panel. (C) Western blots of free 60S subunits isolated from the indicated strains and probed for Rpl3 and Rpl10.

associates with pre-60S particles and known cytoplasmic biogenesis factors Nmd3, Lsg1, and Tif6. Although Reh1 appears to be dispensable when Rei1 is present, when *REI1* is deleted, Reh1 plays a critical role in cellular growth and the formation of mature, stable 60S subunits. We propose that Reh1 and Rei1 have partially redundant functions in cytoplasmic 60S subunit maturation.

What is the nature of the overlapping functions of Reh1/Rei1? Our study shows that the function of Reh1 and the overlapping functions of Reh1 and Rei1 are distinct from Arx1 recycling. Although cytoplasmic Arx1 accumulates in the *reh1*Δ *rei1*Δ strain, the slow growth of this strain is due to an independent defect in ribosome biogenesis as multiple significant defects in growth, polysome levels, subunit joining, and salt stability are not alleviated upon deletion of *ARX1*. Given the evolutionarily conserved nature of Rei1 and the importance of the Arx1-independent overlapping functions of Reh1 and Rei1 in yeast, we expect that Rei1 homologs in other eukaryotes may play important roles in 60S subunit structural stability.

Is it possible that the principal function of Reh1/Rei1 is to recycle a shuttling biogenesis factor other than Arx1? Although our analysis cannot exclude such a possibility, we believe it to be unlikely. We have shown directly that Tif6 recycling is not defective in the *reh1*Δ *rei1*Δ strain. In addition, we found that deletion of both *REH1* and *REI1* does not affect the association of *trans*-acting factors Lsg1, Nmd3, or Tif6 with pre-60S particles. Disruption of recycling of factors that have critical nuclear functions often leads to severe defects in rRNA processing, 60S subunit export, and 60S subunit stoichiometry (12, 29, 32, 35). That we along with others (26) have not observed such phenotypes in cells lacking both Reh1 and Rei1 suggests that the phenotypes observed in cells lacking both

Reh1 and Rei1 do not reflect indirect effects on nuclear steps in 60S subunit assembly or export.

We propose instead that Reh1 and Rei1 directly influence structural rearrangements in the cytoplasmic pre-60S particle, a novel function for a cytoplasmic 60S subunit biogenesis factor. If the pre-60S particle requires a high degree of conformational flexibility to pass through the nuclear pore complex, a concept termed the "baby's head" model (43), Reh1 and Rei1 may act to facilitate the structural rearrangements necessary to adopt a final, structurally stable form.

This study leaves several questions outstanding. Why do yeast cells use functionally redundant proteins Rei1 and Rei1 rather than a single copy of Rei1 (as do most eukaryotes)? What is the specific nature of the 60S subunit conformational change(s) requiring Reh1/Rei1? How does the function of Rei1 in promoting pre-60S particle conformational change relate to its function in recycling Arx1? The resolution of these issues will help us better understand cytoplasmic maturation of the 60S subunit in eukaryotes.

ACKNOWLEDGMENTS

We are grateful to Jonathan Warner (Albert Einstein Medical School, Bronx, NY) for anti-Rpl3 antibody; Bernard Trumpower (Dartmouth Medical School, Hanover, NH) for anti-Rpl10 antibody and the DEH221+ strain; Micheline Fromont-Racine (Pasteur Institute, Paris, France) for anti-Arx1, anti-Rei1, and anti-Rlp24 antibodies and the LMA374 strain; Arlen Johnson (University of Texas, Austin, TX) for anti-Nmd3 antibody and pAJ1004 and pAJ1015 plasmids; Franco Fasiolo (IBMC, Strasbourg, France) for anti-TIF6 antibody; and Heather Hundley for critical reading of the manuscript.

This research was supported by the National Institutes of Health (NRSA postdoctoral fellowship to K.M.P.). B.L.B. is a Howard Hughes Medical Institute Investigator.

REFERENCES

1. **Baronas-Lowell, D. M., and J. R. Warner.** 1990. Ribosomal protein L30 is dispensable in the yeast *Saccharomyces cerevisiae*. Mol. Cell. Biol. **10:**5235–5243.
2. **Basu, U., K. Si, J. R. Warner, and U. Maitra.** 2001. The *Saccharomyces cerevisiae* TIF6 gene encoding translation initiation factor 6 is required for 60S ribosomal subunit biogenesis. Mol. Cell. Biol. **21:**1453–1462.
3. **Baudin, A., O. Ozier-Kalogeropoulos, A. Denouel, F. Lacroute, and C. Cullin.** 1993. A simple and efficient method for direct gene deletion in *Saccharomyces cerevisiae*. Nucleic Acids Res. **21:**3329–3330.
4. **Brachmann, C. B., A. Davies, G. J. Cost, E. Caputo, J. Li, P. Hieter, and J. D. Boeke.** 1998. Designer deletion strains derived from *Saccharomyces cerevisiae* S288C: a useful set of strains and plasmids for PCR-mediated gene disruption and other applications. Yeast **14:**115–132.
5. **Bradatsch, B., J. Katahira, E. Kowalinski, G. Bange, W. Yao, T. Sekimoto, V. Baumgartel, G. Boese, J. Bassler, K. Wild, R. Peters, Y. Yoneda, I. Sinning, and E. Hurt.** 2007. Arx1 functions as an unorthodox nuclear export receptor for the 60S preribosomal subunit. Mol. Cell **27:**767–779.
6. **Dresios, J., I. L. Derkatch, S. W. Liebman, and D. Synetos.** 2000. Yeast ribosomal protein L24 affects the kinetics of protein synthesis and ribosomal protein L39 improves translational accuracy, while mutants lacking both remain viable. Biochemistry **39:**7236–7244.
7. **Eisinger, D. P., F. A. Dick, and B. L. Trumpower.** 1997. Qsr1p, a 60S ribosomal subunit protein, is required for joining of 40S and 60S subunits. Mol. Cell. Biol. **17:**5136–5145.
8. **Fatica, A., and D. Tollervey.** 2002. Making ribosomes. Curr. Opin. Cell Biol. **14:**313–318.
9. **Foiani, M., A. M. Cigan, C. J. Paddon, S. Harashima, and A. G. Hinnebusch.** 1991. GCD2, a translational repressor of the GCN4 gene, has a general function in the initiation of protein synthesis in *Saccharomyces cerevisiae*. Mol. Cell. Biol. **11:**3203–3216.
10. **Fromont-Racine, M., B. Senger, C. Saveanu, and F. Fasiolo.** 2003. Ribosome assembly in eukaryotes. Gene **313:**17–42.
11. **Hartman, H., and A. Fedorov.** 2002. The origin of the eukaryotic cell: a genomic investigation. Proc. Natl. Acad. Sci. USA **99:**1420–1425.
12. **Hedges, J., M. West, and A. W. Johnson.** 2005. Release of the export adapter, Nmd3p, from the 60S ribosomal subunit requires Rpl10p and the cytoplasmic GTPase Lsg1p. EMBO J. **24:**567–579.
13. **Hershey, J. W. B., and M. C. Merrick.** 1996. The pathway and mechanism of eukaryotic protein synthesis, p. 31–69. *In* J. W. B. Hershey, M. B. Mathews, and N. Sonenberg (ed.), Translational control. Cold Spring Harbor Laboratory Press, Cold Spring Harbor, NY.
14. **Ho, J. H., and A. W. Johnson.** 1999. NMD3 encodes an essential cytoplasmic protein required for stable 60S ribosomal subunits in *Saccharomyces cerevisiae*. Mol. Cell. Biol. **19:**2389–2399.
15. **Ho, J. H., G. Kallstrom, and A. W. Johnson.** 2000. Nascent 60S ribosomal subunits enter the free pool bound by Nmd3p. RNA **6:**1625–1634.
16. **Ho, J. H., G. Kallstrom, and A. W. Johnson.** 2000. Nmd3p is a Crm1p-dependent adapter protein for nuclear export of the large ribosomal subunit. J. Cell Biol. **151:**1057–1066.
17. **Hoerz, W., and K. S. McCarty.** 1969. Evidence for a proposed initiation complex for protein synthesis in reticulocyte polyribosome profiles. Proc. Natl. Acad. Sci. USA **63:**1206–1213.
18. **Huh, W. K., J. V. Falvo, L. C. Gerke, A. S. Carroll, R. W. Howson, J. S. Weissman, and E. K. O'Shea.** 2003. Global analysis of protein localization in budding yeast. Nature **425:**686–691.
19. **Hung, N. J., and A. W. Johnson.** 2006. Nuclear recycling of the pre-60S ribosomal subunit-associated factor Arx1 depends on Rei1 in Saccharomyces cerevisiae. Mol. Cell. Biol. **26:**3718–3727.
20. **Hung, N. J., K. Y. Lo, S. S. Patel, K. Helmke, and A. W. Johnson.** 2008. Arx1 is a nuclear export receptor for the 60S ribosomal subunit in yeast. Mol. Biol. Cell **19:**735–744.
21. **Ito, H., Y. Fukuda, K. Murata, and A. Kimura.** 1983. Transformation of intact yeast cells treated with alkali cations. J. Bacteriol. **153:**163–168.
22. **Iwase, M., and A. Toh-e.** 2004. Ybr267w is a new cytoplasmic protein belonging to the mitotic signaling network of *Saccharomyces cerevisiae*. Cell Struct. Funct. **29:**1–15.
23. **Kaiser, C., S. Michaelis, and A. Mitchell.** 1994. Methods in yeast genetics. Cold Spring Harbor Laboratory Press, Cold Spring Harbor, NY.
24. **Kallstrom, G., J. Hedges, and A. Johnson.** 2003. The putative GTPases Nog1p and Lsg1p are required for 60S ribosomal subunit biogenesis and are localized to the nucleus and cytoplasm, respectively. Mol. Cell. Biol. **23:**4344–4355.
25. Reference deleted.
26. **Lebreton, A.** 2006. Ph.D. thesis. Paris 7 University, Pasteur Institute, Paris, France.
27. **Lebreton, A., C. Saveanu, L. Decourty, J. C. Rain, A. Jacquier, and M. Fromont-Racine.** 2006. A functional network involved in the recycling of nucleocytoplasmic pre-60S factors. J. Cell Biol. **173:**349–360.
28. **Longtine, M. S., A. McKenzie III, D. J. Demarini, N. G. Shah, A. Wach, A. Brachat, P. Philippsen, and J. R. Pringle.** 1998. Additional modules for versatile and economical PCR-based gene deletion and modification in *Saccharomyces cerevisiae*. Yeast **14:**953–961.
29. **Menne, T. F., B. Goyenechea, N. Sanchez-Puig, C. C. Wong, L. M. Tonkin, P. J. Ancliff, R. L. Brost, M. Costanzo, C. Boone, and A. J. Warren.** 2007. The Shwachman-Bodian-Diamond syndrome protein mediates translational activation of ribosomes in yeast. Nat. Genet. **39:**486–495.
30. **Meyer, A. E., N. J. Hung, P. Yang, A. W. Johnson, and E. A. Craig.** 2007. The specialized cytosolic J-protein, Jjj1, functions in 60S ribosomal subunit biogenesis. Proc. Natl. Acad. Sci. USA **104:**1558–1563.
31. **Mumberg, D., R. Muller, and M. Funk.** 1995. Yeast vectors for the controlled expression of heterologous proteins in different genetic backgrounds. Gene **156:**119–122.
32. **Pertschy, B., C. Saveanu, G. Zisser, A. Lebreton, M. Tengg, A. Jacquier, E. Liebminger, B. Nobis, L. Kappel, I. van der Klei, G. Hogenauer, M. Fromont-Racine, and H. Bergler.** 2007. Cytoplasmic recycling of 60S preribosomal factors depends on the AAA-protein Drg1. Mol. Cell. Biol. **27:**6581–6592.
33. **Petersen, N., C. S. McLaughlin, and D. P. Nierlich.** 1976. Ribosomal subunit entry into polysomes in yeast. Biochim. Biophys. Acta **447:**294–303.
34. **Saveanu, C., A. Namane, P. E. Gleizes, A. Lebreton, J. C. Rousselle, J. Noaillac-Depeyre, N. Gas, A. Jacquier, and M. Fromont-Racine.** 2003. Sequential protein association with nascent 60S ribosomal particles. Mol. Cell. Biol. **23:**4449–4460.
35. **Senger, B., D. L. Lafontaine, J. S. Graindorge, O. Gadal, A. Camasses, A. Sanni, J. M. Garnier, M. Breitenbach, E. Hurt, and F. Fasiolo.** 2001. The nucle(ol)ar Tif6p and Efl1p are required for a late cytoplasmic step of ribosome synthesis. Mol. Cell **8:**1363–1373.
36. **Si, K., and U. Maitra.** 1999. The *Saccharomyces cerevisiae* homologue of mammalian translation initiation factor 6 does not function as a translation initiation factor. Mol. Cell. Biol. **19:**1416–1426.
37. **Sikorski, R. S., and P. Hieter.** 1989. A system of shuttle vectors and yeast host strains designed for efficient manipulation of DNA in *Saccharomyces cerevisiae*. Genetics **122:**19–27.
38. **Tollervey, D., H. Lehtonen, M. Carmo-Fonseca, and E. C. Hurt.** 1991. The small nucleolar RNP protein NOP1 (fibrillarin) is required for pre-rRNA processing in yeast. EMBO J. **10:**573–583.
39. **Tollervey, D., H. Lehtonen, R. Jansen, H. Kern, and E. C. Hurt.** 1993.

Temperature-sensitive mutations demonstrate roles for yeast fibrillarin in pre-rRNA processing, pre-rRNA methylation, and ribosome assembly. Cell **72:**443–457.
40. **Trapman, J., and R. J. Planta.** 1976. Maturation of ribosomes in yeast. I. Kinetic analysis by labelling of high molecular weight rRNA species. Biochim. Biophys. Acta **442:**265–274.
41. **Tron, T., M. Yang, F. A. Dick, M. E. Schmitt, and B. L. Trumpower.** 1995. QSR1, an essential yeast gene with a genetic relationship to a subunit of the mitochondrial cytochrome bc1 complex, is homologous to a gene implicated in eukaryotic cell differentiation. J. Biol. Chem. **270:**9961–9970.
42. **Tschochner, H., and E. Hurt.** 2003. Pre-ribosomes on the road from the nucleolus to the cytoplasm. Trends Cell Biol. **13:**255–263.
43. **Venema, J., and D. Tollervey.** 1999. Ribosome synthesis in *Saccharomyces cerevisiae*. Annu. Rev. Genet. **33:**261–311.
44. **Warner, J. R.** 1971. The assembly of ribosomes in yeast. J. Biol. Chem. **246:**447–454.